



## Extracellular matrix proteins Pericardin and Lonely heart mediate periostial hemocyte aggregation in the mosquito *Anopheles gambiae*

Cole J. Meier<sup>1</sup>, Shabbir Ahmed<sup>1</sup>, Jordyn S. Barr, Tania Y. Estévez-Lao, Julián F. Hillyer<sup>\*</sup>

Department of Biological Sciences, Vanderbilt University, Nashville, TN, USA

### ARTICLE INFO

**Keywords:**

Hemocyte  
Mosquito immunity  
Heart  
Ostia  
*Anopheles gambiae*  
Extracellular matrix

### ABSTRACT

An infection induces the migration of immune cells called hemocytes to the insect heart, where they aggregate around heart valves called ostia and phagocytose pathogens in areas of high hemolymph flow. Here, we investigated whether the cardiac extracellular matrix proteins, Pericardin (Prc) and Lonely heart (Loh), regulate the infection-induced aggregation of periostial hemocytes in the mosquito, *An. gambiae*. We discovered that RNAi-based post-transcriptional silencing of *Prc* or *Loh* did not affect the resident population of periostial hemocytes in uninfected mosquitoes, but that knocking down these genes decreases the infection-induced migration of hemocytes to the heart. Knocking down *Prc* or *Loh* did not affect the proportional distribution of periostial hemocytes along the periostial regions. Moreover, knocking down *Prc* or *Loh* did not affect the number of sessile hemocytes outside the periostial regions, suggesting that the role of these proteins is cardiac-specific. Finally, knocking down *Prc* or *Loh* did not affect the amount of melanin at the periostial regions, or the intensity of an infection at 24 h after challenge. Overall, we demonstrate that *Prc* and *Loh* are positive regulators of the infection-induced migration of hemocytes to the heart of mosquitoes.

### 1. Introduction

The transmission of mosquito-borne diseases depends on a pathogen's ability to successfully evade the mosquito innate immune system. The immune system of the mosquito can be conceptually divided into cellular and humoral responses (Bartholomay and Michel, 2018; Hillyer, 2010, 2016). The cellular response consists of phagocytosis, whereas the humoral response includes antimicrobial peptides that lyse pathogens, the phenoloxidase cascade that culminates in melanization, reactive oxygen species, and other soluble factors (Bartholomay and Michel, 2018; Hillyer, 2010, 2016; King, 2020; Marmaras and Lampropoulou, 2009; Ratcliffe et al., 2024). At the intersection of cellular and humoral responses lies the hemocyte, which drives both phagocytosis and the production of many humoral effectors (Hillyer and Strand, 2014).

Spatially, hemocytes freely move throughout the hemocoel as circulating hemocytes or are adhered to tissues as sessile hemocytes; this spatial definition, however, is transient because hemocytes can readily alternate between circulating and sessile states (King and Hillyer, 2013; Sigle and Hillyer, 2016, 2018b). About one quarter of the hemocytes in a mosquito are sessile (King and Hillyer, 2013; Sigle and Hillyer, 2016),

and across the insect lineage, a primary site of hemocyte aggregation and immune function is the heart (Yan and Hillyer, 2020). Specifically, a number of resident hemocytes exists attached to the heart, and an infection induces the further aggregation of hemocytes around the ostia that serve as valves for hemolymph entry into the heart (King and Hillyer, 2012; Leodido et al., 2013; Yan and Hillyer, 2020). These hemocytes, known as periostial hemocytes, maximize their chances of encountering a pathogen by aggregating in the regions of the body where hemolymph flow is highest (Sigle and Hillyer, 2016). In fact, periostial hemocytes sequester and phagocytose a disproportionately high amount of pathogens relative to other regions of the body (King and Hillyer, 2012). Similarly, melanin deposition—which indicates that a pathogen has been inactivated via melanization—is highest at the periostial regions, suggesting that either more melanization occurs in these regions, or more likely, that pathogens that are melanized while in circulation are phagocytosed by periostial hemocytes as they are about to flow into the heart (Sigle and Hillyer, 2016; Yassine et al., 2014).

Two major immune pathways—the immune deficiency (IMD) and c-Jun N-terminal kinase (JNK)—drive the infection-induced migration of hemocytes to the heart. Specifically, RNAi-based post-transcriptional

\* Corresponding author. Department of Biological Sciences, Vanderbilt University, VU Station B 35-16342, Nashville, TN, 37235 USA.

E-mail address: [julian.hillyer@vanderbilt.edu](mailto:julian.hillyer@vanderbilt.edu) (J.F. Hillyer).

<sup>1</sup> Contributed equally.

silencing of the transcription factors of the IMD and JNK pathways, *REL2* and *JNK*, reduces the number of periostial hemocytes (Yan et al., 2022b). Conversely, knocking down negative regulators of the IMD pathway, *caspar* and *TGase3*, or the negative regulator of the JNK pathway, *puc*, increases the number of periostial hemocytes (Yan et al., 2022a, 2022b). Other hemocyte-produced factors, such as the members of the Nimrod gene family, Eater and Draper (Sigle and Hillyer, 2018a), or the thioester containing proteins, TEP1 and TEP3 (Yan and Hillyer, 2019), also drive periostial hemocyte aggregation. Considering that infection induces the upregulation of sessile hemocytes on the heart (King and Hillyer, 2012), and that infection reduces the heart rate (Estevez-Lao et al., 2020), it is likely that cardiac components serve as homing signals for the concerted infection-induced arrival of hemocytes to the heart.

In *Drosophila melanogaster* larvae, the cardiac extracellular matrix (ECM) protein, Pericardin (Prc), and its associated receptor, Lonely heart (Loh), are essential for proper heart function and for the developmentally-associated aggregation of hemocytes on the heart (Cevik et al., 2019; Drechsler et al., 2013; Reinhardt et al., 2023). Therefore, we hypothesized that these proteins may play a similar role in mediating the infection-induced aggregation of hemocytes on the heart of adult mosquitoes. In the present study, we identified *Prc* and *Loh* in the genome of the African malaria mosquito, *Anopheles gambiae*, and discovered that they are positive regulators of infection-induced periostial hemocyte aggregation. However, disruption of *Prc* or *Loh* does not alter the proportional distribution of periostial hemocytes across the length of the abdomen, or the mosquito's ability to melanize or otherwise control an infection.

## 2. Methods

### 2.1. Mosquito rearing

*Anopheles gambiae*, Giles sensu stricto (G3 strain; Diptera: Culicidae) were maintained at 27 °C and a relative humidity of 75% with a 12:12hr light:dark photoperiod as described previously (Meier and Hillyer, 2024). Eggs were hatched in deionized water and the larvae fed a koi food and yeast mixture. Adults were fed 10% sucrose ad libitum. Experiments were conducted on adult female mosquitoes.

### 2.2. Bioinformatics analysis

The predicted amino acid sequences for *D. melanogaster* *Prc* (FBgn0028573) and *Loh* (FBgn0032252) were obtained from FlyBase, and used as the query sequence in a BLAST search of the *An. gambiae* PEST genome in VectorBase. For *Prc*, the BLAST search yielded *An. gambiae* AGAP007349 (e-value 5e-107), and reciprocal BLAST search using AGAP007349 as the query sequence returned FBgn0028573. For *Loh*, the BLAST search yielded *An. gambiae* AGAP010003 (e-value 2e-166), and reciprocal BLAST search using AGAP010003 as the query sequence returned FBgn0032252. Amino acid identity was determined by blastp, using the Align Two Sequences tool in NCBI. Orthologs were determined by BLAST in NCBI. Phylogenetic trees were constructed using the MEGA 6.0 and ClustalW program on the amino acid sequence of *Prc* and *Loh* using the maximum likelihood method. To support branch and clustering, bootstrapping values were obtained with 1500 repetitions. For 3D protein structure and superimposition analyses, SWISS-MODEL (<https://swissmodel.expasy.org/>) and UCSF ChimeraX (<https://www.cgl.ucsf.edu/chimerax/>) were utilized.

### 2.3. Synthesis of cDNA and double stranded RNA

Ten mosquito whole bodies were ground and the RNA was purified in TRIzol Reagent (Invitrogen, Carlsbad, CA, USA). RNA was repurified using the RNeasy Mini Kit (Qiagen, Valencia, CA, USA), and up to 5 µg of RNA was then used for cDNA synthesis using an Oligo (dT)<sub>20</sub> primer and

the SuperScript III First-Strand Synthesis System for RT-PCR (Invitrogen) (Yan et al., 2022b).

Gene specific primers containing T7 promoter tags were generated for Pericardin (*Prc*; AGAP007349), Lonely heart (*Loh*; AGAP010030), and Beta-lactamase (*Bla*(*Ap*<sup>R</sup>)). The latter is a gene present in a plasmid of *Escherichia coli* BL21(DE3) cells, and was used as a negative control (Sup. Table S1) (Estevez-Lao and Hillyer, 2014; Yan and Hillyer, 2019; Yan et al., 2022b). Using gene specific primers and *An. gambiae* cDNA or *E. coli* BL21(DE3) lysate as template, amplicons were generated by PCR, separated by agarose gel electrophoresis, excised from gels, and purified using Qiagen's QIAquick Gel Extraction kit. To further increase the amount of dsRNA template, each purified amplicon was used as the template for an additional PCR reaction with the same primers, and up to 1 µg of each purified product was then used as template for dsRNA synthesis using the MEGAscript T7 Kit (Applied Biosystems, Foster City, CA, USA). The dsRNA was ethanol precipitated, re-suspended in phosphate buffer saline (PBS), and the concentration determined spectrophotometrically.

### 2.4. RNAi and bacterial injection

A total of 300 ng of dsRNA was injected at the thoracic anepisternal cleft of 2-day-old mosquitoes using a Nanoject III Programmable Nanoliter Injector (Drummond Scientific, Broomall, PA). Mosquitoes were then transferred to the 27 °C environmental chamber, and 72 h later (so, at 5 days of adulthood), a subset of mosquitoes was intrathoracic injected 69 nl of a bacterial culture. Infections were conducted with GFP-expressing, tetracycline resistant *E. coli* (modified DH5-alpha). Bacterial cultures were grown overnight in Luria–Bertani broth (LB) at 37 °C, diluted to OD<sub>600</sub> of 2, and then injected. Subsequent phenotypic analyses were conducted at 24 h after infection.

### 2.5. Quantification of RNAi knockdown efficiency

At 24 h after immune treatment (naïve and infected), mosquitoes were anesthetized on ice, an incision was made to separate the thorax from the abdomen, and the abdomen was bisected along the coronal plane. The internal organs were then removed from the abdomen, and the dorsal side (containing the heart and other tissues) was transferred to TRIzol Reagent. For each treatment, mRNA from 20 pooled dorsal abdomens was purified using the TRIzol Reagent and repurified with the RNeasy Mini Kit, and up to 3 µg of mRNA was used to synthesize cDNA using the SuperScript III First-Strand Synthesis System for RT-PCR.

To determine RNAi efficiency, qPCR was performed using gene specific primers (Sup. Table S1), the cDNA as template, and Power SYBR Green PCR Master Mix (Applied Biosystems) on a Bio Rad CFX Connect Real-Time Detection System (Hercules, CA, USA). Using the ribosomal protein housekeeping gene, *RpS7*, as a reference, relative mRNA quantification was done using the  $2^{-\Delta\Delta C_t}$  method as previously described (Coggins et al., 2012). The mRNA fold change for both uninfected and infected mosquitoes was calculated relative to the *dsBla*(*Ap*<sup>R</sup>) treatment. Melting curve analysis confirmed the lack of genomic DNA in the cDNA.

### 2.6. Hemocyte staining and dorsal abdomen dissection

At 24 h after immune treatment (naïve and infected), the hemocytes of 6-day old mosquitoes were stained *in vivo* using Vybrant CM-Dil Cell-Labeling Solution (Invitrogen) as previously described, with modification (Fig. 1) (King and Hillyer, 2012). In 27 µL of sterile PBS, 2 µL of 1 mM CM-Dil was combined with 1 µL of 16.2 mM Hoechst 33342 (Invitrogen) and vortexed briefly. Mosquitoes were injected with 200 nL of this solution and allowed to rest for 10 min at room temperature. Mosquitoes were then injected with 200 nL of 16% paraformaldehyde, and following 10 min at room temperature, abdomens were bisected along the coronal plane and transferred to PBS with 0.1% Triton X-100. The dorsal abdomens were then washed with PBS and mounted on a

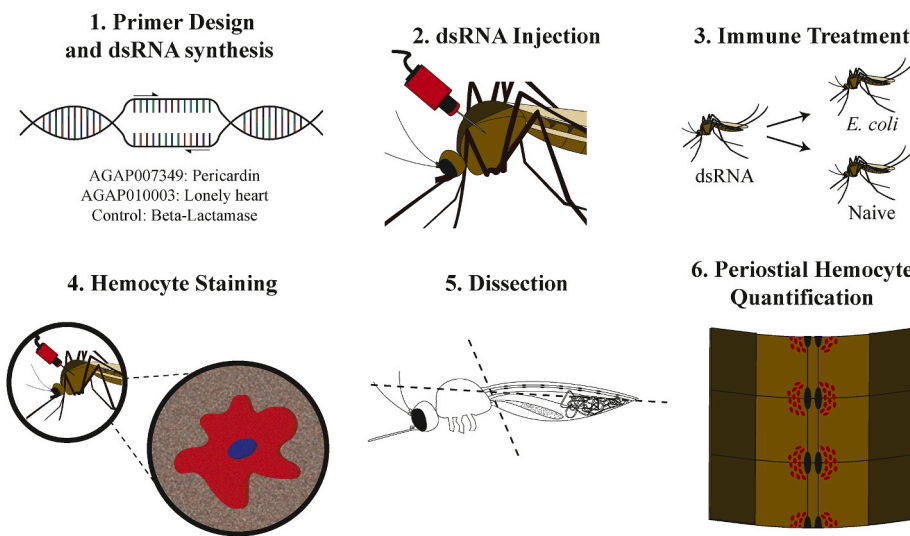


**Fig. 1.** Methodology to determine the effects of Pericardin and Lonely heart on the periostial hemocyte aggregation response.

glass slide with Vectashield Antifade Mounting Media (Vector Laboratories, Newark, CA, USA).

#### 2.7. Imaging and quantification of periostial and sessile hemocytes

Z-stacks at 5  $\mu\text{m}$  steps were taken of the entire dorsal abdomen using both epi-fluorescence and bright field *trans*-illumination using a 10 $\times$  objective on a Nikon Eclipse Ni-E compound microscope and Nikon's Advanced Research NIS Elements software (Nikon, Tokyo, Japan). To quantify the number of hemocytes, all Z-stacks were examined manually, and a cell was determined to be a hemocyte if it was labeled with both CM-Dil (red fluorescence channel) and Hoechst 33342 (blue fluorescence channel), and measured approximately 10–20  $\mu\text{m}$  in diameter (to differentiate them from the much larger pericardial cells and fat body) (Bergmann et al., 2024; Cardoso-Jaime et al., 2023; King and Hillyer, 2012; Sibley and Hillyer, 2016). A hemocyte was classified as 'periostial' if it resided immediately adjacent to the ostia of the mosquito, or within a cluster of hemocytes that touched an ostium. If not, they were classified as 'non-periostial sessile'. Periostial hemocytes were counted for abdominal segments 2–7, whereas non-periostial sessile hemocytes were only counted for abdominal segment 5. Abdominal segment 5 was selected to count non-periostial hemocytes because this is one of the regions of the abdomen with the highest hemolymph flow and contains a significant number of periostial hemocytes (Sibley and Hillyer, 2016, 2018a; Yan and Hillyer, 2019; Yan et al., 2022a).

#### 2.8. Quantification of melanin deposits at the periostial region

Melanin deposition was quantified using the bright field channel of the Z-stacks. Quantification was done for each periostial region of a mosquito using FIJI software. For this, maximum intensity projections from the 10 slices of the Z-stack that were most in focus were first generated. Each image was then processed with the smooth function (1x) tool, and each periostial region was delineated using the square region of interest tool (18,957  $\mu\text{m}^2$ ). Melanin deposits were quantified using a thresholding function that identified the total sum of pixels that were below an intensity threshold that distinguished melanized areas (dark) from non-melanized areas (bright). The threshold range was determined for each trial using a subset of images and held constant across all treatments. Pixels below the threshold that did not clearly correspond to melanin deposits, such as clearly identifiable trachea or setae, were excluded from the analysis. Melanin deposition and hemocyte number were quantified in the same mosquito samples.

#### 2.9. Quantification of *E. coli* infection intensity

Mosquitoes were injected with GFP-expressing, tetracycline resistant *E. coli* (modified DH5-alpha) and incubated at 27 °C and 75% relative humidity for 24 h. Mosquitoes were then homogenized in sterile PBS, the homogenate was diluted 1:500 in sterile PBS, and plated on LB plates containing tetracycline. Plates were grown overnight at 37 °C and colony forming units (CFUs) were screened for GFP fluorescence and counted. The CFU counts and the dilution factor were then used to calculate infection intensity.

#### 2.10. Sampling and statistical analysis

To assay RNAi efficiency, 3 independent trials originating from three different egg batches were conducted; in each trial, each sample consisted of RNA isolated from a pool of 20 dorsal abdomens. To assay periostial hemocytes and melanin deposition, four independent trials were conducted, and in total, a minimum of 15 mosquitoes were analyzed per treatment. The exact number of mosquitoes analyzed for each treatment are presented in the figures. To assay infection intensity, 3 independent trials were conducted, each with 8–10 mosquitoes. Data from all experiments—except infection intensity—were compared via two-way ANOVA, followed by Sídák's post-hoc test. Infection intensity data were compared via a Kruskal-Wallis test. All data collected in this study are presented in [Supplementary Data S1](#).

### 3. Results

#### 3.1. *Prc* and *Loh* in *An. gambiae* and *D. melanogaster* share significant homology

In *D. melanogaster* larva, *Prc* is required for the association of hemocytes to the dorsal vessel during development (Cevik et al., 2019). *Prc* in *D. melanogaster* is a cardiac type IV collagen-like protein that contains an N-terminal signal peptide, several central collagen-like repeat domains (Gly-X-Y)<sub>n</sub>, and can form redox-dependent multimers (Chartier et al., 2002; Drechsler et al., 2013; Hughes and Jacobs, 2017; Reinhardt et al., 2023; Volk et al., 2014; Wilmes et al., 2018). By querying the *An. gambiae* genome, we identified an ortholog of *D. melanogaster Prc*: AGAP007349. The amino acid sequence homology between *An. gambiae Prc* and *D. melanogaster Prc* is 48.15% and the secondary structure of the proteins is also similar—as seen when the predicted crystal structures are superimposed (Fig. 2A). We also identified *Prc* in other insects, and phylogenetic analysis clusters the *An. gambiae Prc* in the same clade as

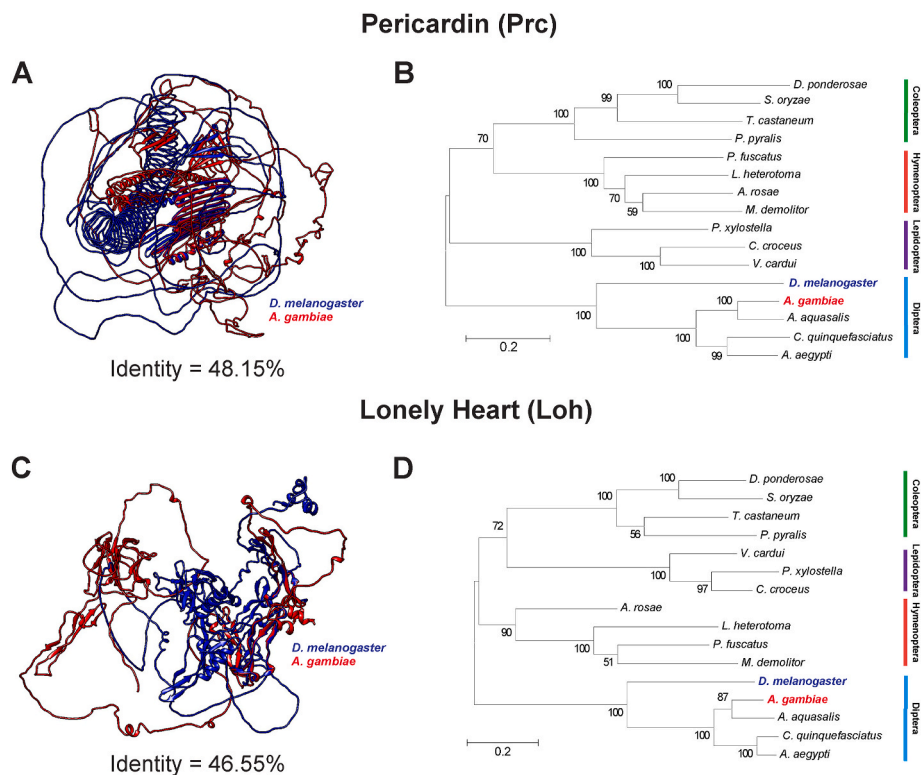


**Fig. 2.** Bioinformatic analysis of Prc and Loh orthologs in *D. melanogaster* and *An. gambiae*. (A) Superimposition of the predicted protein structures of *D. melanogaster* (Blue) and *An. gambiae* (Red) Prc. (B) Prc maximum-likelihood phylogenetic tree. (C) Superimposition of the predicted protein structures of *D. melanogaster* (Blue) and *An. gambiae* (Red) Loh. (D) Loh maximum-likelihood phylogenetic tree. In panels B and D, numbers mark the bootstrap support. (For interpretation of the references to colour in this figure legend, the reader is referred to the Web version of this article.)

Prc from other members of the order Diptera (Fig. 2B; Sup. Table S2).

In *D. melanogaster* larva, Loh is the receptor that specifically recruits Prc to the heart, and therefore, Loh is also required for the association of hemocytes to the dorsal vessel during development (Drechsler et al., 2013). Loh in *D. melanogaster* is a secreted ADAMTS-like protein (a disintegrin-and-metalloprotease-with-thrombospondin-repeats-like protein) containing an N-terminal signal peptide, multiple ADAMTS-1 repeating domains, a spacer region that lacks the proteolytic motif common in ADAMTS proteins, and a Protease and Lacunin (PLAC) domain at the C-terminus (Drechsler et al., 2013; Hughes and Jacobs, 2017; Kuno et al., 1997; Kuno and Matsushima, 1998; Volk et al., 2014). By querying the *An. gambiae* genome, we identified an ortholog of *D. melanogaster* Loh: AGAP010030. The amino acid sequence homology between the *An. gambiae* and *D. melanogaster* Loh is 46.55%, and the predicted secondary structure is similar (Fig. 2C). We also identified Loh in other insects, and phylogenetic analysis clusters *An. gambiae* Loh in the same clade as Loh from other members of the order Diptera (Fig. 2D; Sup. Table S2).

### 3.2. Prc and Loh are positive regulators of periostial hemocyte aggregation following infection

To determine whether Prc or Loh play a role in periostial hemocyte aggregation, we knocked down by RNAi each gene and counted the number of periostial hemocytes in naïve and infected mosquitoes. To measure the efficiency of post-transcriptional silencing, we compared mRNA abundance of *Prc* and *Loh* between mosquitoes injected with either *dsPrc*, *dsLoh*, or the control *dsBla(ApR)*. In naïve mosquitoes, relative mRNA levels of *Prc* and *Loh* were reduced by 75% and 60% relative to the *dsBla(ApR)* treated mosquitoes, respectively. In infected mosquitoes, relative mRNA levels of *Prc* or *Loh* were reduced by 75% and 72%, respectively (Sup. Fig. S1).

We next assessed the number of periostial hemocytes in naïve and infected mosquitoes. Comparison of naïve and infected mosquitoes injected with the negative control dsRNA, *dsBla(ApR)*, showed that infection causes a >5-fold increase in the number of periostial hemocytes (Šídák's Multiple Comparisons Test,  $P_{Bla(ApR):Naive-Bla(ApR):Infected} < 0.0001$ ; Fig. 3). This confirms that infection increases the number of periostial hemocytes. Then, we compared the three dsRNA groups in naïve mosquitoes as well as in infected mosquitoes. In naïve mosquitoes, knocking down of *Prc* or *Loh* did not affect the number of periostial hemocytes relative to *dsBla(ApR)* treated mosquitoes (Šídák's Multiple Comparisons Test,  $P_{Prc:Naive-Bla(ApR):Naive} = 0.9968$  &  $P_{Loh:Naive-Bla(ApR):Naive} = 0.8236$ ). In infected mosquitoes, however, knocking down *Prc* or *Loh* decreased the number of periostial hemocytes by 59% and 61%, respectively, relative to *dsBla(ApR)* treated mosquitoes (Šídák's Multiple Comparisons Test,  $P_{Prc:Infected-Bla(ApR):Infected} < 0.0001$  &  $P_{Loh:Infected-Bla(ApR):Infected} < 0.0001$ ). Despite this RNAi-based decrease in periostial hemocytes, *E. coli* infection still doubled the total number of periostial hemocytes in *dsPrc* and *dsLoh* treated mosquitoes, although this was only statistically significant for *dsPrc* (Šídák's Multiple Comparisons Test,  $P_{Prc:Naive-Prc:Infected} = 0.0127$  &  $P_{Loh:Naive-Loh:Infected} = 0.0924$ ). Altogether, these data demonstrate that knocking down *Prc* or *Loh* does not affect the resident population of periostial hemocytes in naïve mosquitoes, but both genes facilitate the infection-induced migration of hemocytes to the heart.

### 3.3. The proportional distribution of periostial hemocyte aggregation is unaffected by disrupting *Prc* or *Loh*

Hemocytes preferentially aggregate around the ostia in the mid-abdominal segments, which are the segments that experience the most hemolymph flow (Sigle and Hillyer, 2016). Because both Prc and Loh mediate the infection-induced migration of hemocytes to the heart, we

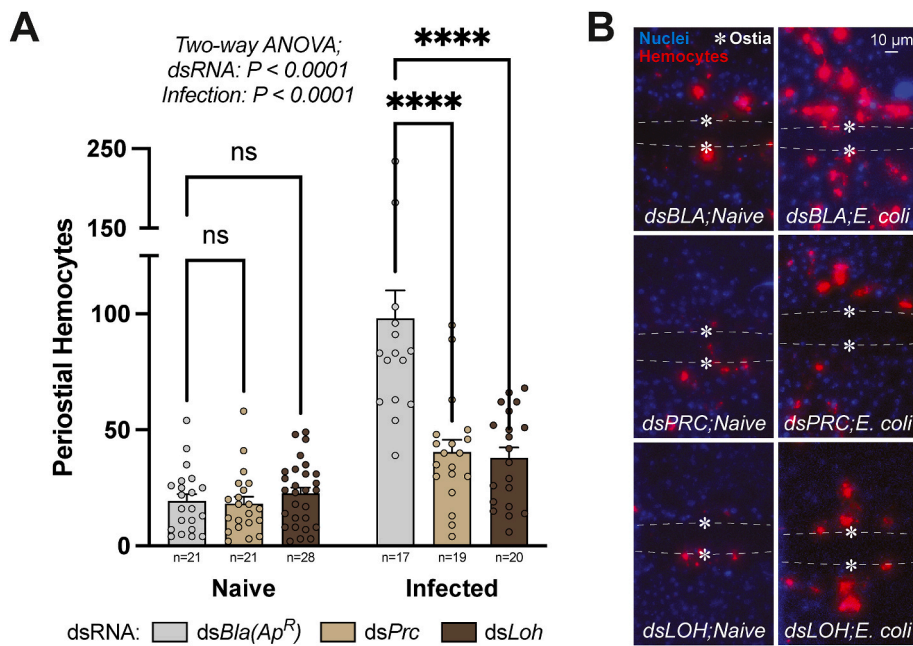


**Fig. 3.** Pericardin and Lonely heart mediate periostial hemocyte aggregation following infection. (A) Average number of periostial hemocytes in naïve and infected mosquitoes that had been treated with dsBla(Ap<sup>R</sup>), dsPrc, or dsLoh. Data were analyzed via 2-way ANOVA, followed by Šídák's Test of multiple comparisons, using dsBla(Ap<sup>R</sup>) as a reference (ns  $P > 0.05$ , \*\*\* $P < 0.0001$ ). Circles denote the value for an individual mosquito, and whiskers denote the S.E.M. (B) Representative fluorescence images of hemocytes (stained red with CM-Dil) around the ostia (asterisks) of abdominal segment 6. Anterior is on the left. Cell nuclei are stained blue with Hoescht 33342. (For interpretation of the references to colour in this figure legend, the reader is referred to the Web version of this article.)

investigated whether knocking down these genes alters the proportional distribution of hemocytes along the periostial regions of abdominal segments 2–7 (Fig. 4). We found that, regardless of immune treatment,

periostial hemocytes are not distributed evenly across abdominal segments in naïve or infected mosquitoes (Two-way ANOVA,  $P_{Naïve:Segment} < 0.0001$  &  $P_{Infected:Segment} < 0.0001$ ), which is in agreement with previous work (Sigle and Hillyer, 2016; Yan and Hillyer, 2019, 2020). More specifically, periostial hemocytes preferentially aggregate in the periostial regions of the mid to posterior abdominal segments. In naïve mosquitoes, dsRNA treatment did not alter the number of periostial hemocytes (Fig. 4A; Two-way ANOVA,  $P_{dsRNA} = 0.1895$ ), but in infected mosquitoes, dsRNA treatment affected the number of periostial hemocytes (Fig. 4B; Two-way ANOVA,  $P_{dsRNA} < 0.0001$ ). This agrees with our analysis of the sum number of periostial hemocytes, which showed that knocking down Prc or Loh does not affect the number of periostial hemocytes in naïve mosquitoes but hampers periostial hemocyte aggregation in infected mosquitoes (Fig. 3). Neither knocking down Prc nor Loh altered the proportional distribution of periostial hemocytes in naïve or infected mosquitoes (Two-way ANOVA,  $P_{Naïve:Interaction} = 0.2210$ ,  $P_{Infected:Interaction} = 0.8105$ ). Altogether, although Prc and Loh are involved in infection-induced periostial hemocyte aggregation, their disruption does not affect the proportional distribution of periostial hemocytes along the abdomen.

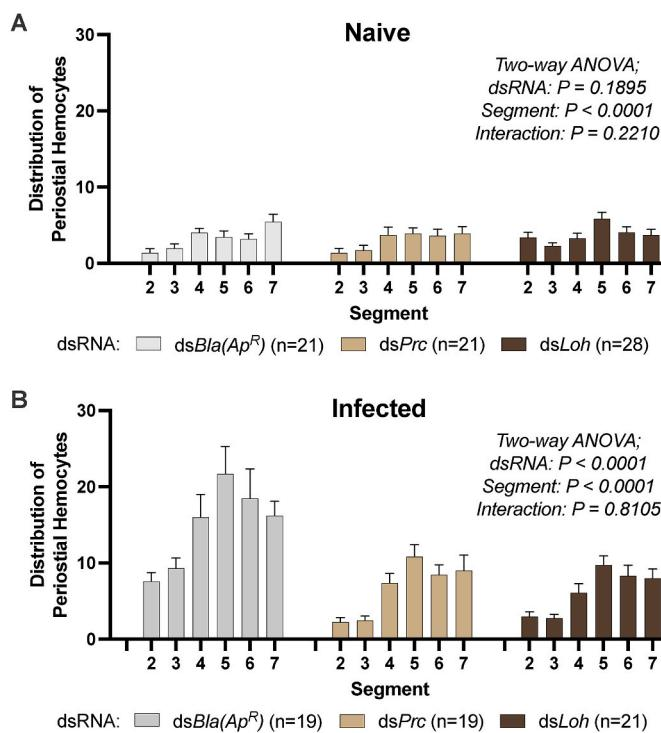


**Fig. 4.** The proportional distribution of periostial hemocytes across abdominal segments is unaffected when pericardin or lonely heart is disrupted. (A–B) The distribution of periostial hemocytes in naïve mosquitoes (A) and mosquitoes 24 h following *E. coli* infection (B) after treatment with dsBla(Ap<sup>R</sup>), dsPrc, or dsLoh. Whiskers represent the SEM. Data were analyzed by two-way ANOVA.

#### 3.4. The number of sessile hemocytes outside the periostial region increases following infection but is unaffected by disrupting Prc or Loh

As hemocytes circulate throughout the mosquito hemocoel, they can attach to any tissue and remain sessile (King and Hillyer, 2012; Sigle and Hillyer, 2016, 2018b). Our first experiment demonstrated that Prc and Loh are positive regulators of infection induced periostial hemocyte aggregation, so we tested whether this phenotype is specific to the heart or whether it applies to all sessile hemocytes by counting the number of non-periostial sessile hemocytes in the dorsal portion of the fifth abdominal segment. Comparison of naïve and infected mosquitoes injected with the negative control dsRNA, dsBla(Ap<sup>R</sup>), showed that infection causes a ~3-fold increase in the number of non-periostial sessile hemocytes (Šídák's Multiple Comparisons Test,  $P_{Bla(ApR):Naïve-Bla(ApR):Infected} = 0.0001$ ; Fig. 5). Next, we compared the effect of Prc and

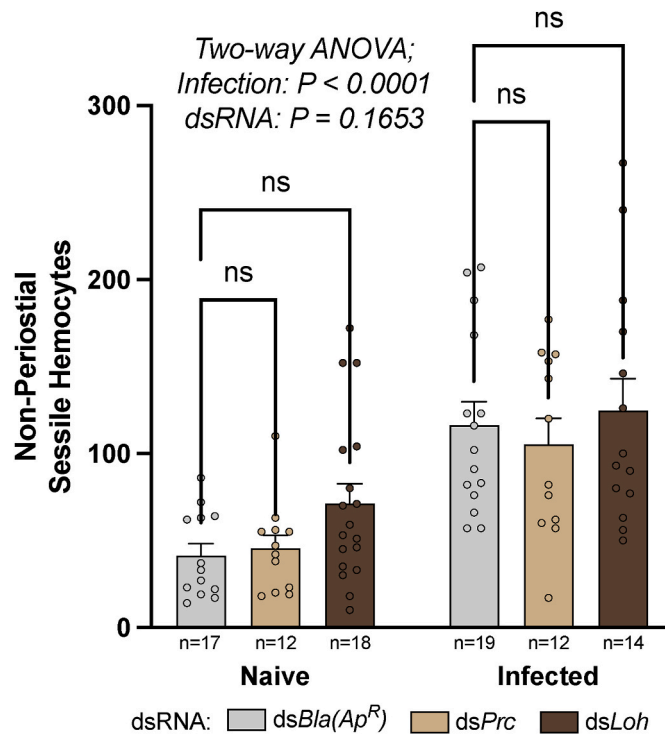


**Fig. 5.** The number of non-periostial sessile hemocytes is unaffected when Pericardin or Lonely heart are disrupted. Average number of sessile hemocytes outside of the periostial region in the fifth abdominal segment of naïve and infected mosquitoes that had been treated with *dsBla(Ap<sup>R</sup>)*, *dsPrc*, or *dsLoh*. Data were analyzed first via a 2-way ANOVA, followed by Šídák's Test of multiple comparisons using *dsBla(Ap<sup>R</sup>)* as a reference (ns,  $P > 0.05$ ). Circles denote the value for an individual mosquito, and whiskers denote the S.E.M.

*Loh* gene knock down in both naïve and infected mosquitoes. In naïve mosquitoes, knocking down *Prc* or *Loh* did not affect the number of non-periostial sessile hemocytes relative to *dsBla(Ap<sup>R</sup>)* (Šídák's Multiple Comparisons Test,  $P_{Prc:\text{Naive-Bla}(Ap^R):\text{Naive}} = 0.9955$  &  $P_{Loh:\text{Naive-Bla}(Ap^R):\text{Naive}} = 0.2573$ ). Similarly, in infected mosquitoes, knocking down *Prc* or

*Loh* did not affect the number of non-periostial sessile hemocytes (Šídák's Multiple Comparisons Test,  $P_{Prc:\text{Infected-Bla}(Ap^R):\text{Infected}} = 0.9135$  &  $P_{Loh:\text{Infected-Bla}(Ap^R):\text{Infected}} = 0.9522$ ). Altogether, although *Prc* and *Loh* facilitate the aggregation of periostial hemocytes following infection, they do not affect the number of sessile hemocytes outside of the periostial regions.

### 3.5. Melanin deposition at the periostial regions is unaffected by disrupting *Prc* or *Loh*

Melanization is a key immune response that sequesters and inactivates pathogens in the hemocoel (Christensen et al., 2005; Whitten and Coates, 2017). Melanin is produced via a proteolytic cascade that is driven by phenoloxidase and other enzymes that are produced by hemocytes (Cerenius and Soderhall, 2021; Hillyer, 2016). Therefore, we investigated whether the decrease in periostial hemocytes that resulted from knocking down *Prc* or *Loh* is accompanied by a similar decrease in melanin deposition at the periostial regions. To do this, we first compared naïve and infected mosquitoes injected with the negative control dsRNA, *dsBla(Ap<sup>R</sup>)*, and found that infection causes a ~10-fold increase in melanin deposition on the heart (Šídák's Multiple Comparisons Test,  $P_{Bla:\text{Naive-Bla}:\text{Infected}} = 0.0173$ ; Fig. 6). Next, we compared the effect of *Prc* and *Loh* gene knock down in naïve and infected mosquitoes. In naïve mosquitoes, knocking down *Prc* or *Loh* did not affect the amount of melanin at the periostial regions relative to *dsBla(Ap<sup>R</sup>)* (Šídák's Multiple Comparisons Test,  $P_{Prc:\text{Naive-Bla}(Ap^R):\text{Naive}} = 0.9865$  &  $P_{Loh:\text{Naive-Bla}(Ap^R):\text{Naive}} = 0.9998$ ). Similarly, in infected mosquitoes, knocking down *Prc* or *Loh* did not affect the amount of melanin at the periostial regions (Šídák's Multiple Comparisons Test,  $P_{Prc:\text{Infected-Bla}(Ap^R):\text{Infected}} = 0.9688$  &  $P_{Loh:\text{Infected-Bla}(Ap^R):\text{Infected}} = 0.0532$ ). Therefore, despite infected mosquitoes with disrupted *Prc* or *Loh* having fewer periostial hemocytes, the melanin deposition within these regions is unchanged.

### 3.6. The intensity of infection is unaffected by disrupting *Prc* or *Loh*

We next investigated whether knocking down *Prc* or *Loh* affects the mosquito's ability to control an infection. To do this, we measured the amount of live *E. coli* present in the hemocoel at 24 h after infection (Fig. 7). Relative to *dsBla(Ap<sup>R</sup>)* mosquitoes, knocking down either *Prc* or

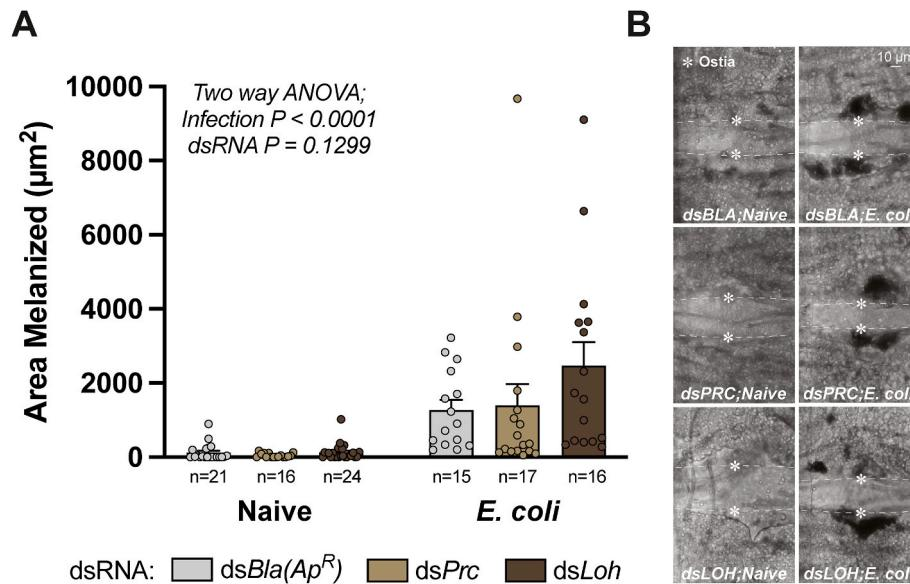


**Fig. 6.** Pericardin and Lonely heart do not affect the amount of melanin deposition at the periostial regions. (A) Average total area of melanin at the periostial regions across abdomen segments 2–7 in naïve and infected mosquitoes that were treated with *dsBla(Ap<sup>R</sup>)*, *dsPrc*, or *dsLoh*. Data were analyzed with a two-way ANOVA. Circles denote the value for an individual mosquito, and whiskers denote the S.E.M. (B) Representative brightfield images of melanin deposition (black) around the ostia of abdominal segment 6.

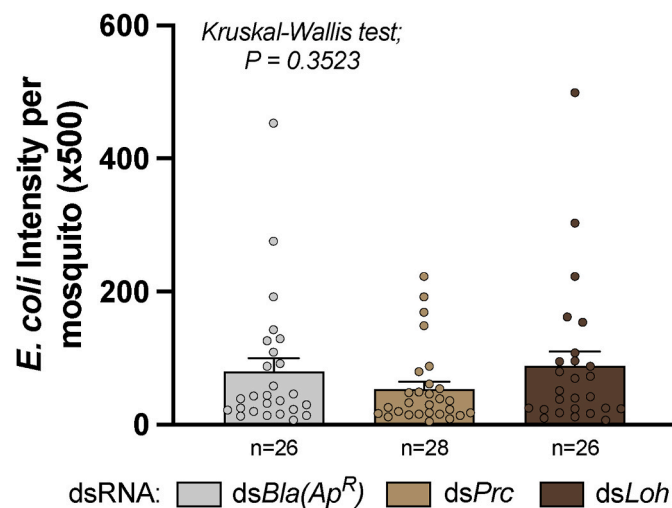


**Fig. 7.** Pericardin and Lonely heart do not affect a mosquito's ability to control a systemic *E. coli* infection. Mean intensity of infection at 24 h following *E. coli* injection in mosquitoes treated with *dsBla(Ap<sup>R</sup>)*, *dsPrc*, or *dsLoh*. Each data point represents the infection intensity in an individual mosquito. Data were analyzed with a Kruskal-Wallis test. Circles denote the value for an individual mosquito, and whiskers denote the S.E.M.

*Loh* did not affect the intensity of infection (Kruskal-Wallis,  $P = 0.3523$ ). Therefore, *Prc* or *Loh* are not required for the control of a systemic *E. coli* infection.

#### 4. Discussion

The aggregation of hemocytes to the periostial region is an immune response that is conserved across insects (Hillyer and Pass, 2020; King and Hillyer, 2012; Yan and Hillyer, 2020). Prior work identified immune pathways that regulate this aggregation response (Sigle and Hillyer, 2018a; Yan and Hillyer, 2019; Yan et al., 2022a, 2022b), but heart specific factors that serve as homing signals for hemocytes migrating to the mosquito heart were unknown. Here, we demonstrate that the cardiac extracellular matrix protein, Pericardin, and its associated receptor, Lonely heart, mediate the infection-induced periostial hemocyte response in adult *An. gambiae* (Fig. 8). RNAi-based post-transcriptional silencing of *Prc* or *Loh* decreases the number of periostial hemocytes following an infection. This reduction does not affect the proportional distribution of periostial hemocytes across the abdomen, the amount of melanin deposited at the periostial region, or the strength of the systemic immune response.

The ECM is a network of proteins and polysaccharides that form a scaffolding which connects and protects tissues and organs (Frantz et al., 2010; Hughes and Jacobs, 2017; Kular et al., 2014). The ECM is comprised of a basement membrane that garners tensile strength to the cell and provides an interactive interface between the cell and its surroundings, and an interstitial space that is a gel-like matrix that occupies and fills the area within the ECM (Hughes and Jacobs, 2017; Kular et al.,

2014; Yurchenco, 2011). *Prc* is a basement membrane protein within the cardiac ECM of *D. melanogaster* that is restricted to the dorsolateral region of the heart (Cevik et al., 2019; Chartier et al., 2002; Drechsler et al., 2013; Hughes and Jacobs, 2017; Sessions et al., 2017). *Prc*, like other *D. melanogaster* collagen-type IV proteins, is critical for cardiac integrity during heart development and plays a role in adhesion between cardiac cells (Cevik et al., 2019; Chartier et al., 2002; Drechsler et al., 2013; Hollfelder et al., 2014; Hughes and Jacobs, 2017). During *D. melanogaster* embryogenesis, *Prc* is expressed by pericardial cells (Chartier et al., 2002), but in larvae and adults, *Prc* is expressed in the fat body (Drechsler et al., 2013; Gera et al., 2022; Reinhardt et al., 2023). In adulthood, JNK and p38 signal the release of cytokine unpaired 3 (Upd3) from pericardial nephrocytes during infection, which in turn upregulates *Prc* in the fat body. (Gera et al., 2022; Reinhardt et al., 2023). Here, we demonstrate that, in adult mosquitoes, *Prc* is a positive regulator of the infection-induced aggregation of periostial hemocytes. Given that the JNK pathway positively regulates periostial hemocyte aggregation in *An. gambiae* (Yan et al., 2022b), a possible mechanism is that the JNK pathway drives the production of *Prc*, thereby creating a heart environment that is more attractive to the adherence of hemocytes that are circulating.

*Loh* is a secreted ADAMTS-like protein that controls the localization of *Prc* to the abluminal region of the heart (Cevik et al., 2019; Drechsler et al., 2013; Hughes and Jacobs, 2017; Volk et al., 2014). *Loh* controls the cardiac-specific distribution of *Prc*, and therefore, is essential for cardiac integrity during *D. melanogaster* development (Drechsler et al., 2013). The exact mechanism by which *Loh* recruits *Prc* to the heart is unclear, but in *D. melanogaster*, ectopic expression of *Loh* on muscle tissue is sufficient to recruit *Prc* and induce the binding of hemocytes to that muscle (Cevik et al., 2019). Here, we discovered that *Loh*, like *Prc*, mediates the infection-induced periostial hemocyte aggregation response in adult mosquitoes. We suspect that without *Loh* or *Prc*, the circulating hemocytes that pass by the ECM that surrounds the heart's ostia are less likely to adhere and remove themselves from circulation.

Following a bloodmeal (Bryant and Michel, 2014, 2016; Castillo et al., 2011), or infection (Christensen et al., 1989; King and Hillyer, 2013), hemocytes undergo mitotic proliferation and their number increases. With infection resulting in more hemocytes, *Prc* or *Loh* could mediate the specific aggregation of hemocytes on the heart, or the more general binding of hemocytes to any tissue. Here, we discovered that *Prc* and *Loh* mediate hemocyte aggregation at the periostial regions but not in non-periostial regions of the abdomen. This finding identifies the cardiac ECM as a critical component of the mechanism by which hemocytes specifically aggregate to the periostial regions in response to infection. Because infection still doubles the number of periostial hemocytes in *dsPrc* treated mosquitoes, other cardiac-specific ECM components may also mediate periostial hemocyte aggregation. Alternatively, this increase may be due to the residual *Prc* remaining on the heart following an incomplete knockdown via dsRNA treatment. Furthermore, knocking down *Prc* or *Loh* does not decrease the number of resident periostial hemocytes in naïve mosquitoes. This implies that other cardiac proteins could be facilitating the basal adhesion of resident periostial hemocytes, or that the resident population of periostial hemocytes from the moment of dsRNA treatment to the moment of analysis

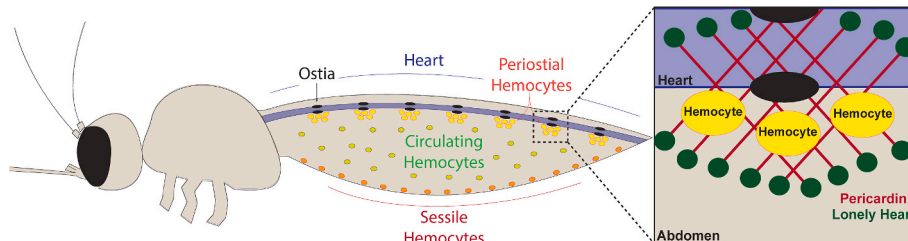


**Fig. 8.** Pericardin and Lonely heart are positive regulators of periostial hemocyte aggregation in mosquitoes.

is stable.

In mosquitoes, melanization is an important immune response that is mediated by hemocytes (Christensen et al., 2005; Hillyer, 2010). Two of the functional sub-classes of the *An. gambiae* hemocyte, the granulocyte and the oenocytoid, contribute to melanization at varying degrees. Granulocytes are the primary phagocytic cells whereas oenocytoids are the primary producers of pro-phenoloxidase and other enzymes that drive the melanization biochemical cascade (Castillo et al., 2006; Hillyer and Christensen, 2005; Hillyer et al., 2003a). Despite the role of hemocytes in melanization, a reduced periostial hemocyte immune response following the knockdown of *Prc* and *Loh* did not affect the amount of melanin in the periostial regions following infection. It has previously been hypothesized that, because small melanized pathogens are phagocytosed (Hillyer et al., 2003a), the accumulation of melanin in the periostial regions is from the phagocytosis of already melanized bacteria by periostial hemocytes (Sible and Hillyer, 2016). It is possible that the resident population of periostial hemocytes is sufficient to phagocytose the melanized bacteria that are circulating, especially because melanization is not a primary mechanism used by mosquitoes to kill *E. coli* (Hillyer et al., 2003b).

Because of the destructive nature of the infection intensity experiment (whole bodies were ground and plated), we could not calculate whether there was a correlation between infection intensity and the number of periostial hemocytes. However, the number of periostial hemocytes increases further when the infection dose is increased (King and Hillyer, 2012). Therefore, we predict that, regardless of RNAi treatment, mosquitoes with a higher infection intensity are likely to have more periostial hemocytes.

Following exposure to a pathogen, mosquitoes mount a variety of immune responses to mitigate the escalation of an infection (Bartholomay and Michel, 2018; Hillyer, 2010, 2016; Marmaras and Lamproulou, 2009; Ratcliffe et al., 2024). Here, we found that the infection intensity of mosquitoes exposed to *E. coli* did not differ between mosquitoes treated with ds*Prc* or ds*Loh*, relative to mosquitoes treated with ds*Bla(Ap<sup>R</sup>)*—despite ameliorating the periostial hemocyte immune response. Disrupting *Prc* or *Loh* impairs hemocyte localization and not the ability of mosquitoes to be immunocompetent. Therefore, for this type of infection, the basal periostial hemocyte population may be sufficient to conduct the requisite immune function on the heart, in concert with the function of circulating hemocytes and other immune mechanisms.

## 5. Conclusion

Periostial hemocytes lie at the crux of the cellular and humoral immune responses that protect the mosquito from pathogens (Hillyer and Strand, 2014). Multiple immune effectors regulate the aggregation of hemocytes on the heart (Sible and Hillyer, 2018a; Yan and Hillyer, 2019; Yan et al., 2022a, 2022b). Here, we demonstrate that in addition to these immune effectors, the ECM—and specifically pericardin and lonely heart—is a critical component in the infection-induced migration of hemocytes to the heart.

## CRediT authorship contribution statement

**Cole J. Meier:** Writing – review & editing, Writing – original draft, Visualization, Validation, Methodology, Investigation, Formal analysis, Data curation, Conceptualization. **Shabbir Ahmed:** Writing – review & editing, Validation, Methodology, Investigation, Formal analysis, Conceptualization. **Jordyn S. Barr:** Writing – review & editing, Methodology, Investigation, Conceptualization. **Tania Y. Estévez-Lao:** Writing – review & editing, Investigation, Formal analysis. **Julian F. Hillyer:** Writing – review & editing, Writing – original draft, Visualization, Supervision, Resources, Project administration, Methodology, Funding acquisition, Formal analysis, Data curation, Conceptualization.

## Data availability

All data generated or analyzed during this study are included in this published article and its supplementary information files.

## Acknowledgments

We thank Lindsay Martin for helpful discussions and feedback on the manuscript. This work was funded by National Science Foundation (NSF) Grant IOS-1949145 to JFH.

## Appendix A. Supplementary data

Supplementary data to this article can be found online at <https://doi.org/10.1016/j.dci.2024.105219>.

## References

- Bartholomay, L.C., Michel, K., 2018. Mosquito immunobiology: the intersection of vector health and vector competence. *Annu. Rev. Entomol.* 63, 145–167.
- Bergmann, S., Graf, E., Hoffmann, P., Becker, S.C., Stern, M., 2024. Localization of nitric oxide-producing hemocytes in *Aedes* and *Culex* mosquitoes infected with bacteria. *Cell Tissue Res.* 395, 313–326.
- Bryant, W.B., Michel, K., 2014. Blood feeding induces hemocyte proliferation and activation in the African malaria mosquito, *Anopheles gambiae* Giles. *J. Exp. Biol.* 217, 1238–1245.
- Bryant, W.B., Michel, K., 2016. *Anopheles gambiae* hemocytes exhibit transient states of activation. *Dev. Comp. Immunol.* 55, 119–129.
- Cardoso-Jaime, V., Maya-Maldonado, K., Tsutsumi, V., Hernandez-Martinez, S., 2023. Mosquito pericardial cells upregulate Cecropin expression after an immune challenge. *Dev. Comp. Immunol.* 147, 104745.
- Castillo, J., Brown, M.R., Strand, M.R., 2011. Blood feeding and insulin-like peptide 3 stimulate proliferation of hemocytes in the mosquito *Aedes aegypti*. *PLoS Pathog.* 7, e1002274.
- Castillo, J.C., Robertson, A.E., Strand, M.R., 2006. Characterization of hemocytes from the mosquitoes *Anopheles gambiae* and *Aedes aegypti*. *Insect Biochem. Mol. Biol.* 36, 891–903.
- Cerenius, L., Soderhall, K., 2021. Immune properties of invertebrate phenoloxidases. *Dev. Comp. Immunol.* 122, 104098.
- Cevik, D., Acker, M., Michalski, C., Jacobs, J.R., 2019. Pericardin, a *Drosophila* collagen, facilitates accumulation of hemocytes at the heart. *Dev. Biol.* 454, 52–65.
- Chartier, A., Zaffran, S., Astier, M., Semeriva, M., Gratecos, D., 2002. Pericardin, a *Drosophila* type IV collagen-like protein is involved in the morphogenesis and maintenance of the heart epithelium during dorsal ectoderm closure. *Development* 129, 3241–3253.
- Christensen, B.M., Huff, B.M., Miranpuri, G.S., Harris, K.L., Christensen, L.A., 1989. Hemocyte population changes during the immune response of *Aedes aegypti* to inoculated microfilariae of *Dirofilaria immitis*. *J. Parasitol.* 75, 119–123.
- Christensen, B.M., Li, J., Chen, C.C., Nappi, A.J., 2005. Melanization immune responses in mosquito vectors. *Trends Parasitol.* 21, 192–199.
- Coggins, S.A., Estevez-Lao, T.Y., Hillyer, J.F., 2012. Increased survivorship following bacterial infection by the mosquito *Aedes aegypti* as compared to *Anopheles gambiae* correlates with increased transcriptional induction of antimicrobial peptides. *Dev. Comp. Immunol.* 37, 390–401.
- Drechsler, M., Schmidt, A.C., Meyer, H., Paululat, A., 2013. The conserved ADAMTS-like protein lonely heart mediates matrix formation and cardiac tissue integrity. *PLoS Genet.* 9, e1003616.
- Estevez-Lao, T.Y., Hillyer, J.F., 2014. Involvement of the *Anopheles gambiae* Nimrod gene family in mosquito immune responses. *Insect Biochem. Mol. Biol.* 44, 12–22.
- Estevez-Lao, T.Y., Sible, L.T., Gomez, S.N., Hillyer, J.F., 2020. Nitric oxide produced by periostial hemocytes modulates the bacterial infection-induced reduction of the mosquito heart rate. *J. Exp. Biol.* 223, jeb225821.
- Frantz, C., Stewart, K.M., Weaver, V.M., 2010. The extracellular matrix at a glance. *J. Cell Sci.* 123, 4195–4200.
- Gera, J., Budakoti, P., Suhag, M., Mandal, L., Mandal, S., 2022. Physiological ROS controls Upd3-dependent modeling of ECM to support cardiac function in *Drosophila*. *Sci. Adv.* 8, eabj4991.
- Hillyer, J.F., 2010. Mosquito immunity. *Adv. Exp. Med. Biol.* 708, 218–238.
- Hillyer, J.F., 2016. Insect immunology and hematopoiesis. *Dev. Comp. Immunol.* 58, 102–118.
- Hillyer, J.F., Christensen, B.M., 2005. Mosquito phenoloxidase and defensin colocalize in melanization innate immune responses. *J. Histochem. Cytochem.* 53, 689–698.
- Hillyer, J.F., Pass, G., 2020. The insect circulatory system: structure, function, and evolution. *Annu. Rev. Entomol.* 65, 121–143.
- Hillyer, J.F., Schmidt, S.L., Christensen, B.M., 2003a. Hemocyte-mediated phagocytosis and melanization in the mosquito *Armigeres subalbatus* following immune challenge by bacteria. *Cell Tissue Res.* 313, 117–127.
- Hillyer, J.F., Schmidt, S.L., Christensen, B.M., 2003b. Rapid phagocytosis and melanization of bacteria and *Plasmodium* sporozoites by hemocytes of the mosquito *Aedes aegypti*. *J. Parasitol.* 89, 62–69.

Hillyer, J.F., Strand, M.R., 2014. Mosquito hemocyte-mediated immune responses. *Curr Opin Insect Sci* 3, 14–21.

Hollfelder, D., Frasch, M., Reim, I., 2014. Distinct functions of the laminin beta LN domain and collagen IV during cardiac extracellular matrix formation and stabilization of alary muscle attachments revealed by EMS mutagenesis in *Drosophila*. *BMC Dev. Biol.* 14, 26.

Hughes, C.J.R., Jacobs, J.R., 2017. Dissecting the role of the extracellular matrix in heart disease: lessons from the *Drosophila* genetic model. *Vet Sci* 4, 24.

King, J.G., 2020. Developmental and comparative perspectives on mosquito immunity. *Dev. Comp. Immunol.* 103, 103458.

King, J.G., Hillyer, J.F., 2012. Infection-induced interaction between the mosquito circulatory and immune systems. *PLoS Pathog.* 8, e1003058.

King, J.G., Hillyer, J.F., 2013. Spatial and temporal in vivo analysis of circulating and sessile immune cells in mosquitoes: hemocyte mitosis following infection. *BMC Biol.* 11, 55.

Kular, J.K., Basu, S., Sharma, R.I., 2014. The extracellular matrix: structure, composition, age-related differences, tools for analysis and applications for tissue engineering. *J. Tissue Eng.* 5, 2041731414557112.

Kuno, K., Kanada, N., Nakashima, E., Fujiki, F., Ichimura, F., Matsushima, K., 1997. Molecular cloning of a gene encoding a new type of metalloproteinase-disintegrin family protein with thrombospondin motifs as an inflammation associated gene. *J. Biol. Chem.* 272, 556–562.

Kuno, K., Matsushima, K., 1998. ADAMTS-1 protein anchors at the extracellular matrix through the thrombospondin type I motifs and its spacing region. *J. Biol. Chem.* 273, 13912–13917.

Leodido, A.C.M., Ramalho-Ortigao, M., Martins, G.F., 2013. The ultrastructure of the *Aedes aegypti* heart. *Arthropod Struct. Dev.* 42, 539–550.

Marmaras, V.J., Lampropoulou, M., 2009. Regulators and signalling in insect haemocyte immunity. *Cell. Signal.* 21, 186–195.

Meier, C.J., Hillyer, J.F., 2024. Larvicidal activity of the photosensitive insecticides, methylene blue and rose bengal, in *Aedes aegypti* and *Anopheles gambiae* mosquitoes. *Pest Manag. Sci.* 80, 296–306.

Ratcliffe, N.A., Mello, C.B., Castro, H.C., Dyson, P., Figueiredo, M., 2024. Immune reactions of vector insects to parasites and pathogens. *Microorganisms* 12, 568.

Reinhardt, M., Drechsler, M., Paululat, A., 2023. *Drosophila* collagens in specialised extracellular matrices. *Biol. Chem.* 404, 535–550.

Sessions, A.O., Kaushik, G., Parker, S., Raedschelders, K., Bodmer, R., Van Eijk, J.E., Engler, A.J., 2017. Extracellular matrix downregulation in the *Drosophila* heart preserves contractile function and improves lifespan. *Matrix Biol.* 62, 15–27.

Sigle, L.T., Hillyer, J.F., 2016. Mosquito hemocytes preferentially aggregate and phagocytose pathogens in the periostial regions of the heart that experience the most hemolymph flow. *Dev. Comp. Immunol.* 55, 90–101.

Sigle, L.T., Hillyer, J.F., 2018a. Eater and draper are involved in the periostial haemocyte immune response in the mosquito *Anopheles gambiae*. *Insect Mol. Biol.* 27, 429–438.

Sigle, L.T., Hillyer, J.F., 2018b. Mosquito hemocytes associate with circulatory structures that support intracardiac retrograde hemolymph flow. *Front. Physiol.* 9, 1187.

Volk, T., Wang, S., Rotstein, B., Paululat, A., 2014. Matricellular proteins in development: perspectives from the *Drosophila* heart. *Matrix Biol.* 37, 162–166.

Whitten, M.M.A., Coates, C.J., 2017. Re-evaluation of insect melanogenesis research: views from the dark side. *Pigment Cell Melanoma Res* 30, 386–401.

Wilmes, A.C., Klinke, N., Rotstein, B., Meyer, H., Paululat, A., 2018. Biosynthesis and assembly of the collagen IV-like protein pericardin in *Drosophila melanogaster*. *Biol. Open* 7, bio030361.

Yan, Y., Hillyer, J.F., 2019. Complement-like proteins TEP1, TEP3 and TEP4 are positive regulators of periostial hemocyte aggregation in the mosquito *Anopheles gambiae*. *Insect Biochem. Mol. Biol.* 107, 1–9.

Yan, Y., Hillyer, J.F., 2020. The immune and circulatory systems are functionally integrated across insect evolution. *Sci. Adv.* 6, eabb3164.

Yan, Y., Ramakrishnan, A., Estevez-Lao, T.Y., Hillyer, J.F., 2022a. Transglutaminase 3 negatively regulates immune responses on the heart of the mosquito, *Anopheles gambiae*. *Sci. Rep.* 12, 6715.

Yan, Y., Sigle, L.T., Rinker, D.C., Estevez-Lao, T.Y., Capra, J.A., Hillyer, J.F., 2022b. The immune deficiency and c-Jun N-terminal kinase pathways drive the functional integration of the immune and circulatory systems of mosquitoes. *Open Biol* 12, 220111.

Yassine, H., Kamareddine, L., Chamat, S., Christophides, G.K., Osta, M.A., 2014. A serine protease homolog negatively regulates TEP1 consumption in systemic infections of the malaria vector *Anopheles gambiae*. *J. Innate Immun.* 6, 806–818.

Yurchenco, P.D., 2011. Basement membranes: cell scaffoldings and signaling platforms. *Cold Spring Harbor Perspect. Biol.* 3, a004911.